Cell Metabolism, Volume *26*

Supplemental Information

Hypothalamic AMPK-ER Stress-JNK1 Axis Mediates the Central Actions of Thyroid Hormones on Energy Balance

Noelia Martínez-Sánchez, Patricia Seoane-Collazo, Cristina Contreras, Luis Varela, Joan Villarroya, Eva Rial-Pensado, Xabier Buqué, Igor Aurrekoetxea, Teresa C. Delgado, Rafael Vázquez-Martínez, Ismael González-García, Juan Roa, Andrew J. Whittle, Beatriz Gomez-Santos, Vidya Velagapudi, Y.C. Loraine Tung, Donald A. Morgan, Peter J. Voshol, Pablo B. Martínez de Morentin, Tania López-González, Laura Liñares-Pose, Francisco Gonzalez, Krishna Chatterjee, Tomás Sobrino, Gema Medina-Gómez, Roger J. Davis, Núria Casals, Matej Orešič, Anthony P. Coll, Antonio Vidal-Puig, Jens Mittag, Manuel Tena-Sempere, María M. Malagón, Carlos Diéguez, María Luz Martínez-Chantar, Patricia Aspichueta, Kamal Rahmouni, Rubén Nogueiras, Guadalupe Sabio, Francesc Villarroya, and Miguel López

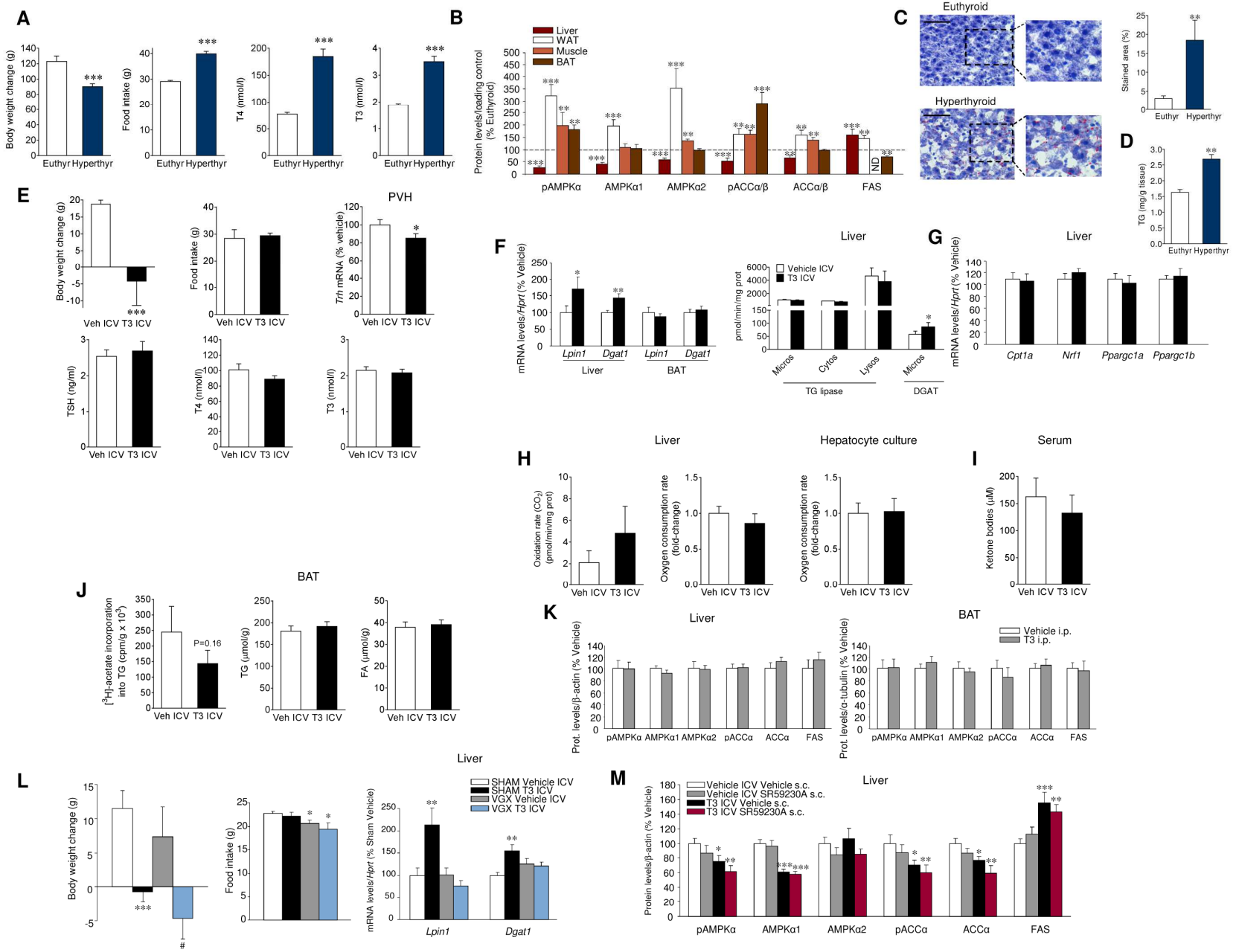
A
Body weight change (g)
Food intake (g)
T4 (nmol/l)
T3 (nmol/l)
Euthyr Hyperthyr
B
Liver
WAT
Muscle
BAT
Protein levels/loading control (% Euthyroid)
pAMPKα
AMPKα1
AMPKα2
pACCα/β
ACCα/β
FAS
ND
C
Euthyroid
Hyperthyroid
Stained area (%)
D
TG (mg/g tissue)
E
PVH
Body weight change (g)
Veh ICV T3 ICV
Food intake (g)
Trh mRNA (% vehicle)
TSH (ng/ml)
T4 (nmol/l)
T3 (nmol/l)
F
mRNA levels/Hprt (% Vehicle)
Lpin1
Dgat1
Liver
BAT
pmol/min/mg prot
Vehicle ICV
T3 ICV
Micros
Cytos
Lysos
TG lipase
DGAT
G
Liver
Cpt1a
Nrf1
Ppargc1a
Ppargc1b
H
Liver
Hepatocyte culture
Oxidation rate (CO2) (pmol/min/mg prot)
Oxygen consumption rate (fold-change)
I
Serum
Ketone bodies (μM)
J
BAT
[3H]-acetate incorporation into TG (cpm/g x 10^3)
P=0.16
TG (μmol/g)
FA (μmol/g)
K
Liver
BAT
Vehicle i.p.
T3 i.p.
Prot. levels/β-actin (% Vehicle)
Prot. levels/α-tubulin (% Vehicle)
pAMPKα
AMPKα1
AMPKα2
pACCα
ACCα
FAS
L
Liver
SHAM Vehicle ICV
SHAM T3 ICV
VGX Vehicle ICV
VGX T3 ICV
Body weight change (g)
Food intake (g)
mRNA levels/Hprt (% Sham Vehicle)
Lpin1
Dgat1
M
Liver
Vehicle ICV Vehicle s.c.
Vehicle ICV SR59230A s.c.
T3 ICV Vehicle s.c.
T3 ICV SR59230A s.c.
Protein levels/β-actin (% Vehicle)

FIGURE S1 related to Figure 1. Effect of peripheral or central TH on liver and BAT metabolism

(A) Body weight change, daily food intake, circulating levels of T4 and T3 of euthyroid and hyperthyroid rats (n=9-18 rats/group).

(B) Protein levels of the AMPK pathway in the liver, WAT, muscle and BAT of euthyroid and hyperthyroid rats. Data are expressed as a percentage of controls for each tissue. In this sense, to simplify the graphs, the control bars have been omitted and the control level (100%) represented as a dotted line. In the ACC analyses the data shown ACCα for liver, WAT and BAT and ACCβ for the muscle. In the muscle samples, as expected, FAS expression was non-detected (ND) (n=8-17 rats/group).

(C) Representative Oil Red O images (left panel; 20x; scale bar: 100 μm), staining analysis (right panel) and **(D)** triglyceride (TG) levels in the liver of euthyroid and hyperthyroid rats (n=10-18 rats/group).

(E) Body weight change, daily food intake, TRH mRNA levels in the paraventricular nucleus of the hypothalamus (PVH) and circulating levels of TSH, T4 and T3 of rats ICV treated with vehicle or T3 (n=9-11 rats/group; 7 for the mRNA analysis).

(F) *Lpin* and *Dgat1* mRNA levels in the liver and BAT (left panel), microsomal, cytosolic and lysosomal TG lipase and DGAT activities (right panel) and **(G)** lipid oxidative gene expression in the liver of rats ICV treated with vehicle or T3 (n=8-10 rats/group; 5 rats/group were assayed).

(H) Lipid oxidation rate (left panel), oxygen consumption rate (middle panel) in the liver and oxygen consumption in hepatocyte cultures (right panel), **(I)** circulating ketone bodies of rats ICV treated with vehicle or T3 (n=4-5 rats/group).

(J) [^{3}H]-acetate incorporation into TG (left panel), TG levels (middle panel) and FA levels (right panel) in the BAT of rats ICV treated with vehicle or T3 (n=6-10 animals), (**K**) protein levels of the AMPK pathway in the liver (left panel) and BAT (right panel) of rats with intraperitoneal (i.p.) administration of T3 at the same dose used ICV (n=7-10 rats/group).

(L) Body weight change (left panel), daily food intake (middle panel) and *Lpin* and *Dgat1* mRNA levels in the liver (right panel) of sham and vagotomized (VGX) rats ICV treated with vehicle or T3 (n=13-14 rats/group; 9 for the mRNA analysis).

(M) Protein levels of AMPK pathway in the liver of rats ICV treated with vehicle or T3 and s.c. treated with the β3-AR specific antagonist SR59230A (n=7 rats/group).

**P*<0.05, ***P*<0.01, ****P*<0.001 *vs.* euthyroid, vehicle ICV, sham vehicle ICV, vehicle ICV vehicle s.c. All data are expressed as mean±SEM.

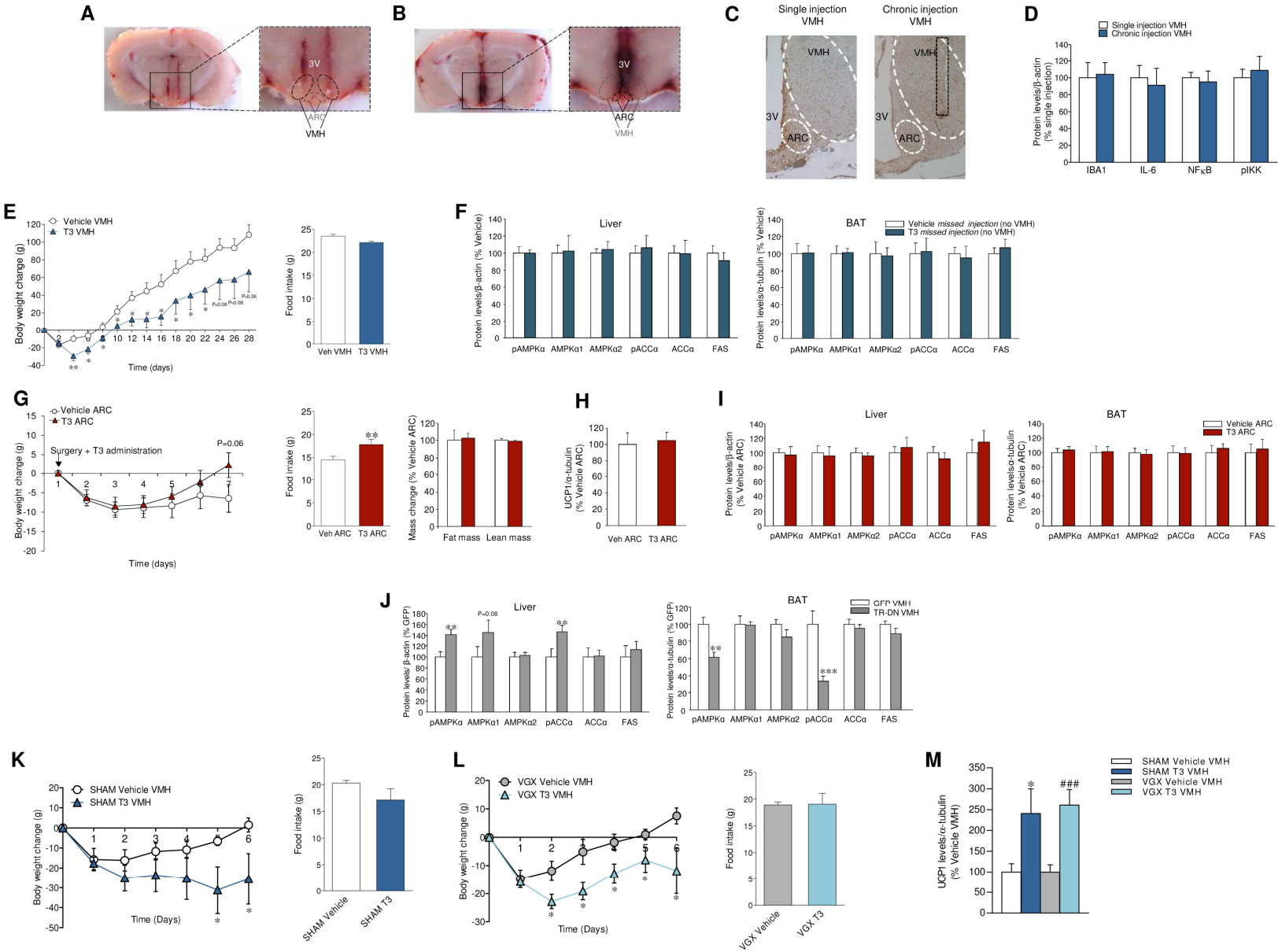
A
3V
ARC
VMH
B
3V
ARC
VMH
C
Single injection VMH
Chronic injection VMH
VMH
3V
ARC
D
Single injection VMH
Chronic injection VMH
Protein levels/β-actin (% single injection)
IBA1
IL-6
NFκB
pIKK
E
Vehicle VMH
T3 VMH
Body weight change (g)
Time (days)
P=0.06
P=0.08
P=0.08
Food intake (g)
Veh VMH
T3 VMH
F
Liver
BAT
Vehicle missed injection (no VMH)
T3 missed injection (no VMH)
Protein levels/β-actin (% Vehicle)
Protein levels/α-tubulin (% Vehicle)
pAMPKα
AMPKα1
AMPKα2
pACCα
ACCα
FAS
G
Vehicle ARC
T3 ARC
Surgery + T3 administration
P=0.06
Body weight change (g)
Time (days)
Food intake (g)
Veh ARC
T3 ARC
Mass change (% Vehicle ARC)
Fat mass
Lean mass
H
UCP1/α-tubulin (% Vehicle ARC)
Veh ARC
T3 ARC
I
Liver
BAT
Vehicle ARC
T3 ARC
Protein levels/β-actin (% Vehicle ARC)
Protein levels/α-tubulin (% Vehicle ARC)
J
Liver
BAT
GFP VMH
TR-DN VMH
Protein levels/β-actin (% GFP)
Protein levels/α-tubulin (% GFP)
P=0.08
K
SHAM Vehicle VMH
SHAM T3 VMH
Body weight change (g)
Time (Days)
Food intake (g)
SHAM Vehicle
SHAM T3
L
VGX Vehicle VMH
VGX T3 VMH
Body weight change (g)
Time (Days)
Food intake (g)
VGX Vehicle
VGX T3
M
SHAM Vehicle VMH
SHAM T3 VMH
VGX Vehicle VMH
VGX T3 VMH
UCP1 levels/α-tubulin (% Vehicle VMH)

FIGURE S2 related to Figure 2. Effect of VMH T3 on liver and BAT metabolism

(A) Histological images of coronal sections of the rat brains showing the localization of the cannulae in the ventromedial (VMH) and **(B)** arcuate (ARC) nuclei of the hypothalamus.

(C) Immunoreactivity of IBA1 and **(D)** protein levels of inflammatory markers in the VMH from single or chronic injection in the VMH (n=6-7 rats/group).

(E) Body weight change (left panel) and daily food intake (right panel) of rats and chronically treated in the VMH with vehicle or T3 (n=9 rats/group).

(F) Protein levels of the AMPK pathway in liver (left panel) and BAT (right panel) of rats receiving T3 *"missed"* injections in *"VMH neighboring areas"* (n=7 rats/group).

(G) Body weight (left panel), daily food intake (middle panel) and mass change (right panel) of rats treated in the ARC with vehicle or T3 (n=9 rats/group).

(H) Protein levels of UCP1 in BAT and **(I)** the AMPK pathway in liver (left panel) and BAT (right panel) of rats treated in the ARC with vehicle or T3 (n=7 rats/group).

(J) Protein levels the AMPK pathway in liver (left panel) and BAT (right panel) of rats treated in the VMH with adenovirus encoding GFP or a dominant negative mutant of thyroid hormone receptor (TR-DN) (n=7 rats/group).

(K) Body weight change (left panels) and **(L)** daily food intake (right panels) of sham and vagotomized (VGX) rats treated in the VMH with vehicle or T3 (n=7-8 rats/group).

(M) Protein levels of UCP1 in BAT of sham and VGX rats treated in the VMH with vehicle or T3 (n=7 rats/group).

$*P<0.05$, $**P<0.01$, $***P<0.001$ *vs.* vehicle VMH, vehicle ARC. GFP or sham vehicle VMH; ### $P<0.001$ *vs.* VGX Vehicle VMH. All data are expressed as mean±SEM.

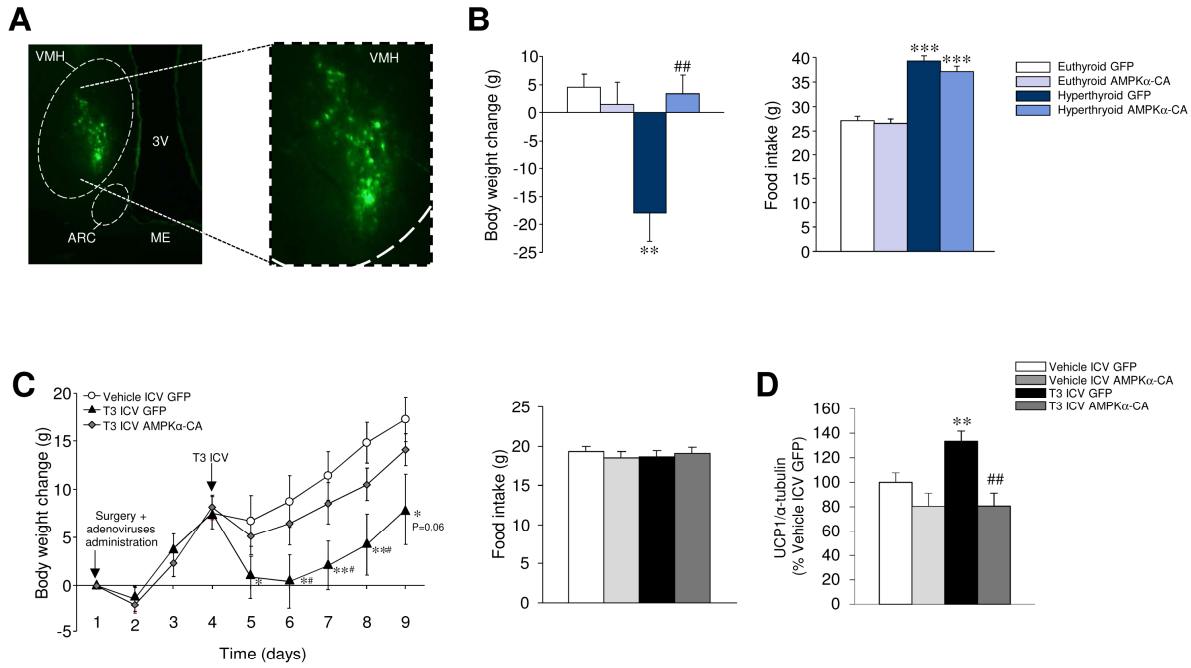

FIGURE S3 related to Figure 3. Effect of AMPK in the VMH on the central actions of THs on liver and BAT metabolism

(A) Direct fluorescence of GFP (left: 4x, right: 20x) in the ventromedial nucleus of the hypothalamus (VMH) of rats treated in the VMH with adenoviruses encoding GFP.

(B) Body weight change (left panel) and daily food intake (right panel) of euthyroid and hyperthyroid rats treated in the VMH with adenoviruses encoding GFP or a constitutive active mutant of AMP-activated protein kinase alpha (AMPKα-CA) (n=17-24 rats/group).

(C) Body weight change (left panel) and daily food intake (right panel) of rats ICV treated with vehicle or T3 and treated in the VMH with adenoviruses encoding GFP or AMPKα-CA (n=7 rats/group).

(D) Protein levels of UCP1 in BAT of rats ICV treated with vehicle or T3 and treated in the VMH with adenovirus encoding GFP or AMPKα-CA (n=7 rats/group).

**P*<0.05, ***P*<0.01, ****P*<0.001 *vs.* euthyroid GFP or vehicle ICV GFP; #*P*<0.05, ##*P*<0.01 *vs.* hyperthyroid GFP or T3 ICV GFP. All data are expressed as mean±SEM.

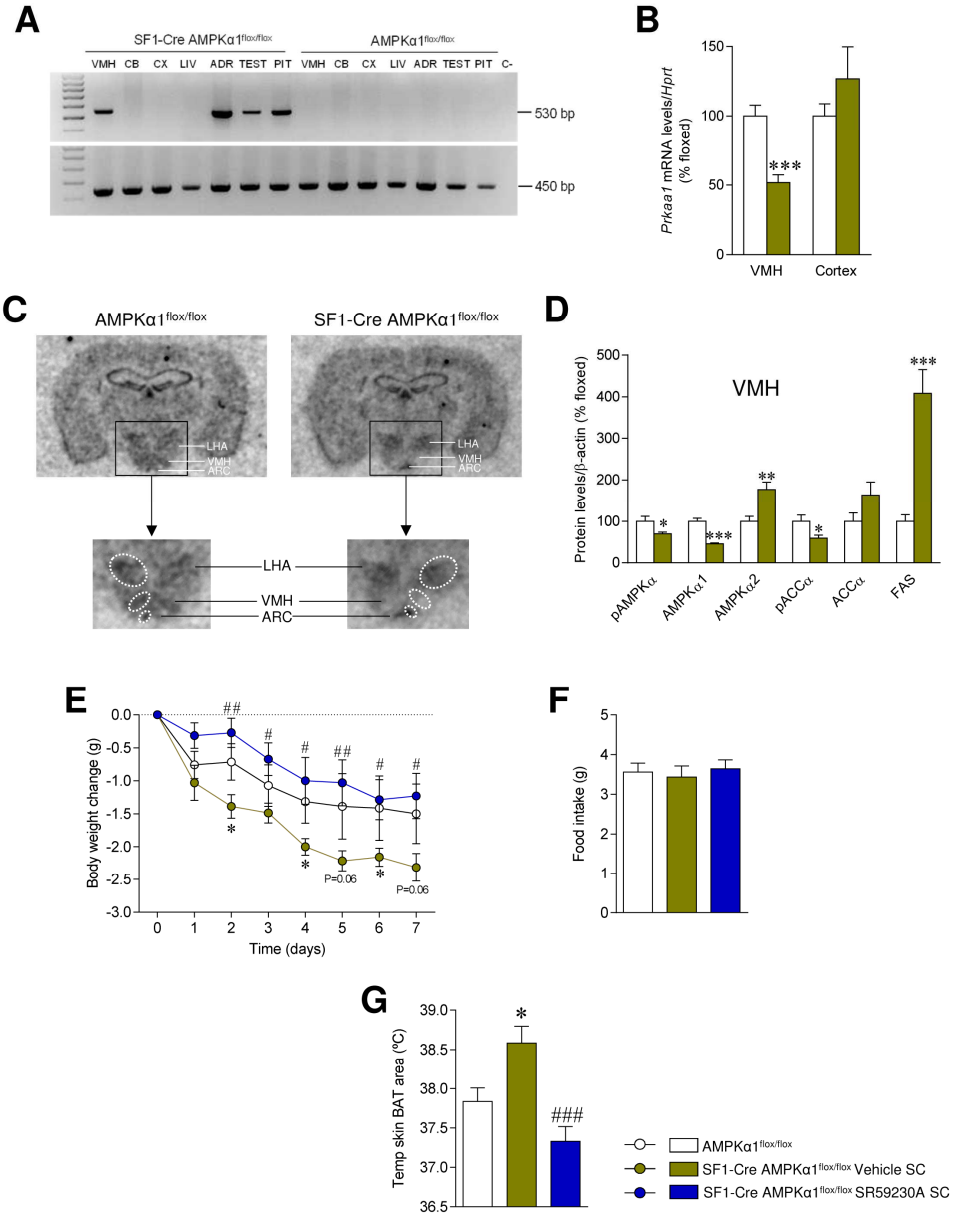

FIGURE S4 related to Figure 4. Validation of the deletion of AMPKα1 in SF1 neurons and effect of β3-AR blockage

(A) PCR genotyping using samples from the ventromedial nucleus of the hypothalamus (VMH), cerebellum (CB), cortex (CX), liver (LIV), adrenal gland (ADR), testes (TEST), pituitary (PIT) of SF1-Cre AMPKα1$^{flox/flox}$ and AMPKα1$^{flox/flox}$ mice. C-: negative control.

(B) *Prkaa1* mRNA levels in the VMH and cortex of SF1-Cre AMPKα1$^{flox/flox}$ and AMPKα1$^{flox/flox}$ mice (n=8 mice/group).

(C) Representative *in situ* hybridization images obtained with an oligo against *Prkaa1* in SF1-Cre AMPKα1$^{flox/flox}$ and AMPKα1$^{flox/flox}$ mice. The magnification shows the hypothalamus, where positive signal is found in the arcuate nucleus (ARC) and the VMH, as well as in the lateral hypothalamic area (LHA) of AMPKα1$^{flox/flox}$ mice. In the SF1-Cre AMPKα1$^{flox/flox}$ no signal is found in the VMH.

(D) Protein levels of the AMPK pathway in the VMH of SF1-Cre AMPKα1$^{flox/flox}$ and AMPKα1$^{flox/flox}$ mice (n=7 mice/group).

(E) Body weight change, **(F)** food intake and **(G)** temperature of BAT skin area of AMPKα1$^{flox/flox}$ mice and SF1-Cre AMPKα1$^{flox/flox}$ mice s.c. treated with vehicle or the β3-AR specific antagonist SR59230A (n=7 mice/group).

**P*<0.05, ***P*<0.01, ****P*<0.001 *vs.* AMPKα1$^{flox/flox}$; #P<0.05, ##P<0.01 and ###*P*<0.001 *vs.* SF1-Cre AMPKα1$^{flox/flox}$ vehicle s.c. All data are expressed as mean±SEM.

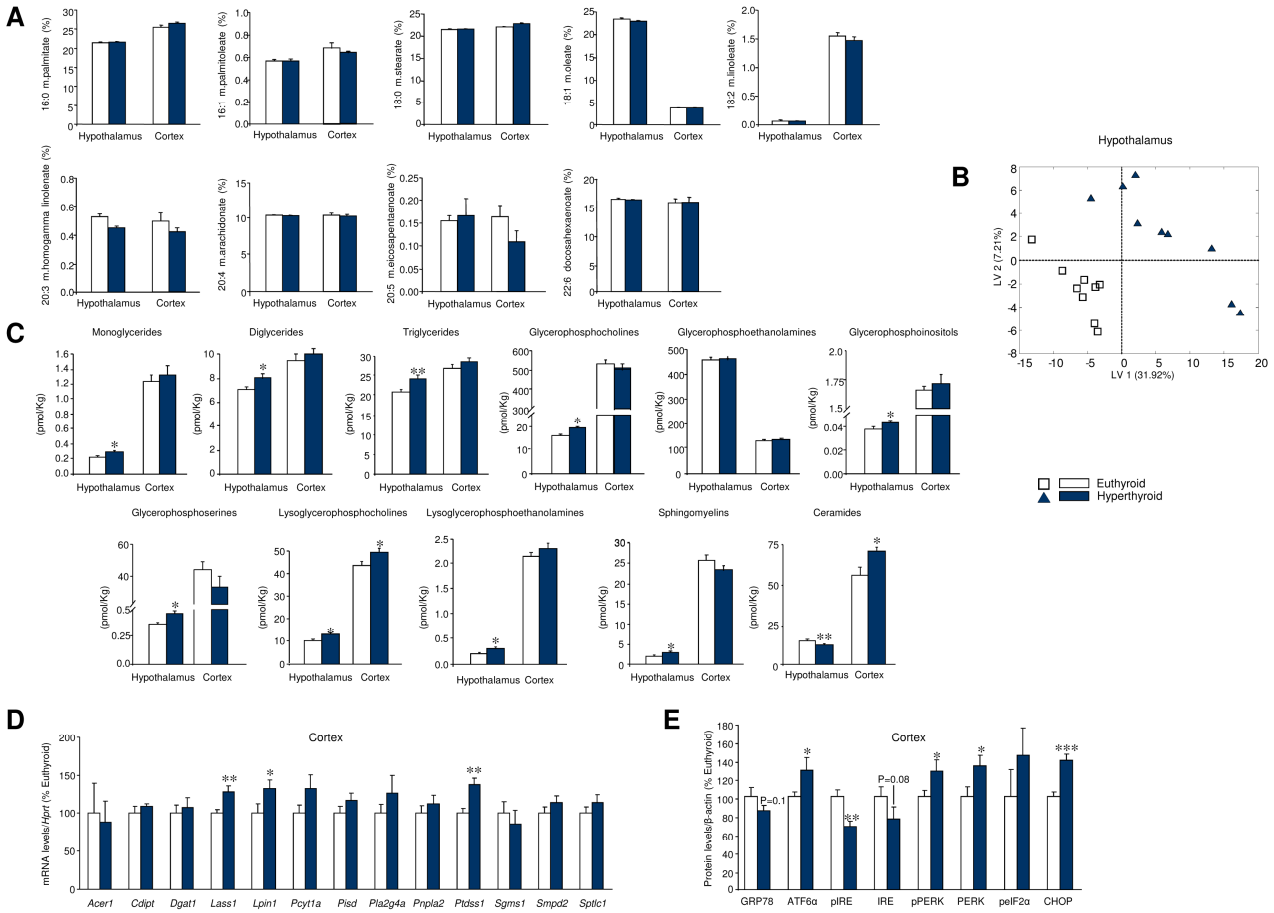

FIGURE S5 related to Figure 5. Effect of THs on hypothalamic lipid composition

(A) Fatty acid composition, **(B)** comparative multivariate analysis, **(C)** levels of lipid species in hypothalamus and cortex of euthyroid and hyperthyroid rats (n=9 rats/group).

(D) mRNA levels of enzymes involved in metabolism of complex lipids and **(E)** protein levels of the UPR in the cortex of euthyroid and hyperthyroid rats (n=7-8 rats/group).

**P*<0.05, ***P*<0.01, ****P*<0.001 *vs.* euthyroid. All data are expressed as mean±SEM.

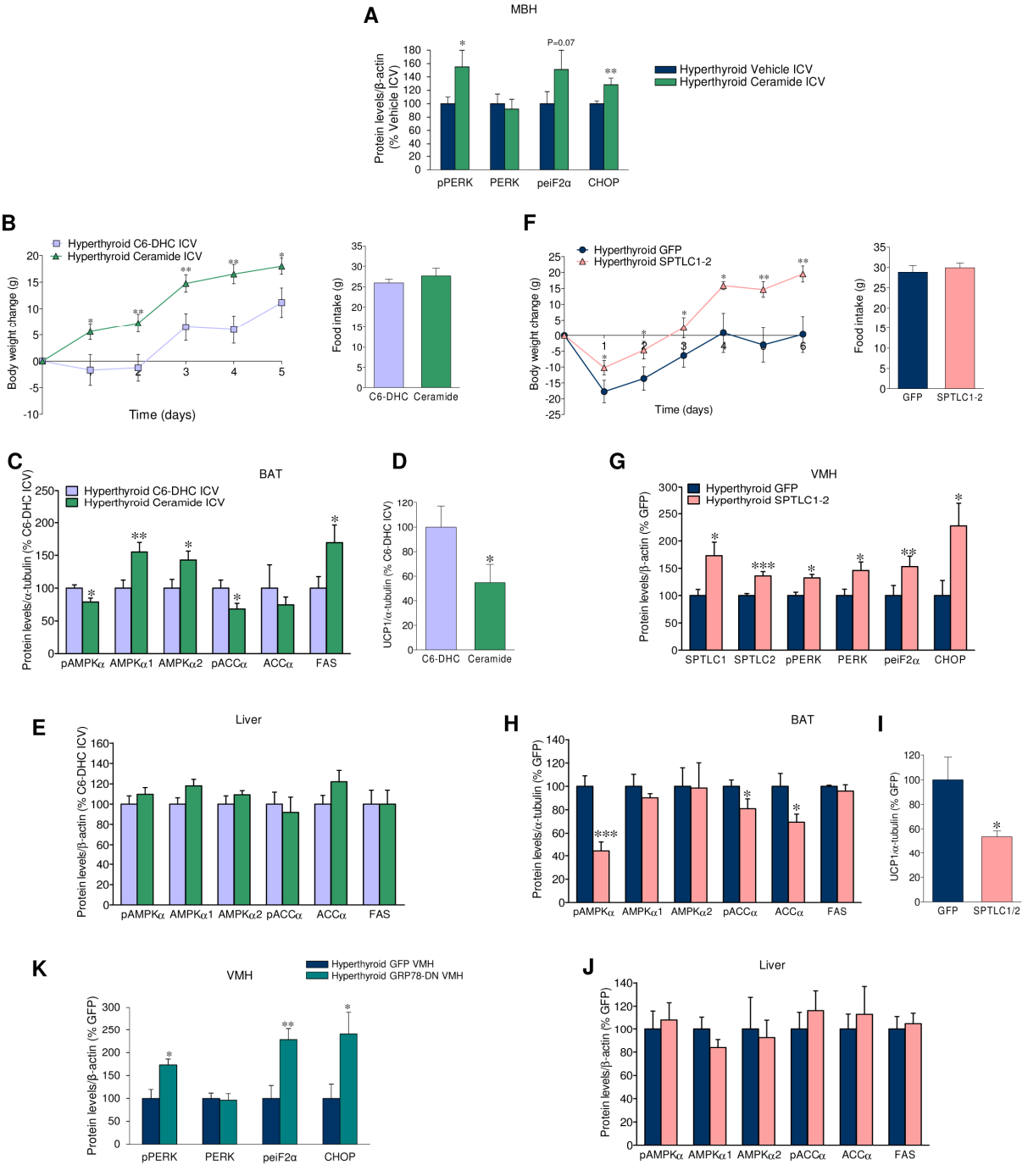

FIGURE S6 related to Figure 6. Effect of hypothalamic ceramides pathway on the central actions of THs on liver and BAT metabolism

(A) Protein levels of the UPR in the mediobasal hypothalamus (MBH) in hyperthyroid rats ICV treated with a vehicle or C6 ceramide (n=8-9 rats/group).

(B) Body weight change (left panel) and daily food intake (right panel) of hyperthyroid rats ICV treated with C6 ceramide or C6-dihydroceramide (C6-DHC) (n=8-9 rats/group).

(C-E) Protein levels of the AMPK pathway in the BAT **(C)**, UCP1 in the BAT **(D)** and the AMPK pathway in the liver **(E)** of hyperthyroid rats ICV treated with C6 ceramide or C6-dihydroceramide (C6-DHC) (n=7 rats/group).

(F) Body weight change (left panel) and daily food intake (right panel) of hyperthyroid rats treated in the ventromedial nucleus of the hypothalamus (VMH) with adenoviruses encoding GFP or serine palmitoyltransferase, long chain subunit 1-2 (SPTLC1-2) (n=8-9 rats/group).

(G-J) Protein levels of SPTCL1-2 and the UPR in the hypothalamus **(G),** the AMPK pathway in the BAT **(H)**, UCP1 in the BAT **(I)** and the AMPK pathway in the liver **(J)** of hyperthyroid rats treated in the VMH with adenoviruses encoding GFP or SPTLC1-2 (n=7 rats/group).
(K) Protein levels of the UPR in the VMH of hyperthyroid rats treated in the VMH with adenoviruses encoding GFP or a dominant negative mutant of glucose regulated protein 78 KDa (GRP78-DN) (n=7-14 rats/group).
**P*<0.05, ***P*<0.01, ****P*<0.001 *vs* Hyperthyroid vehicle ICV, Hyperthyroid C6-DHC ICV and Hyperthyroid GFP. All data are expressed as mean±SEM.

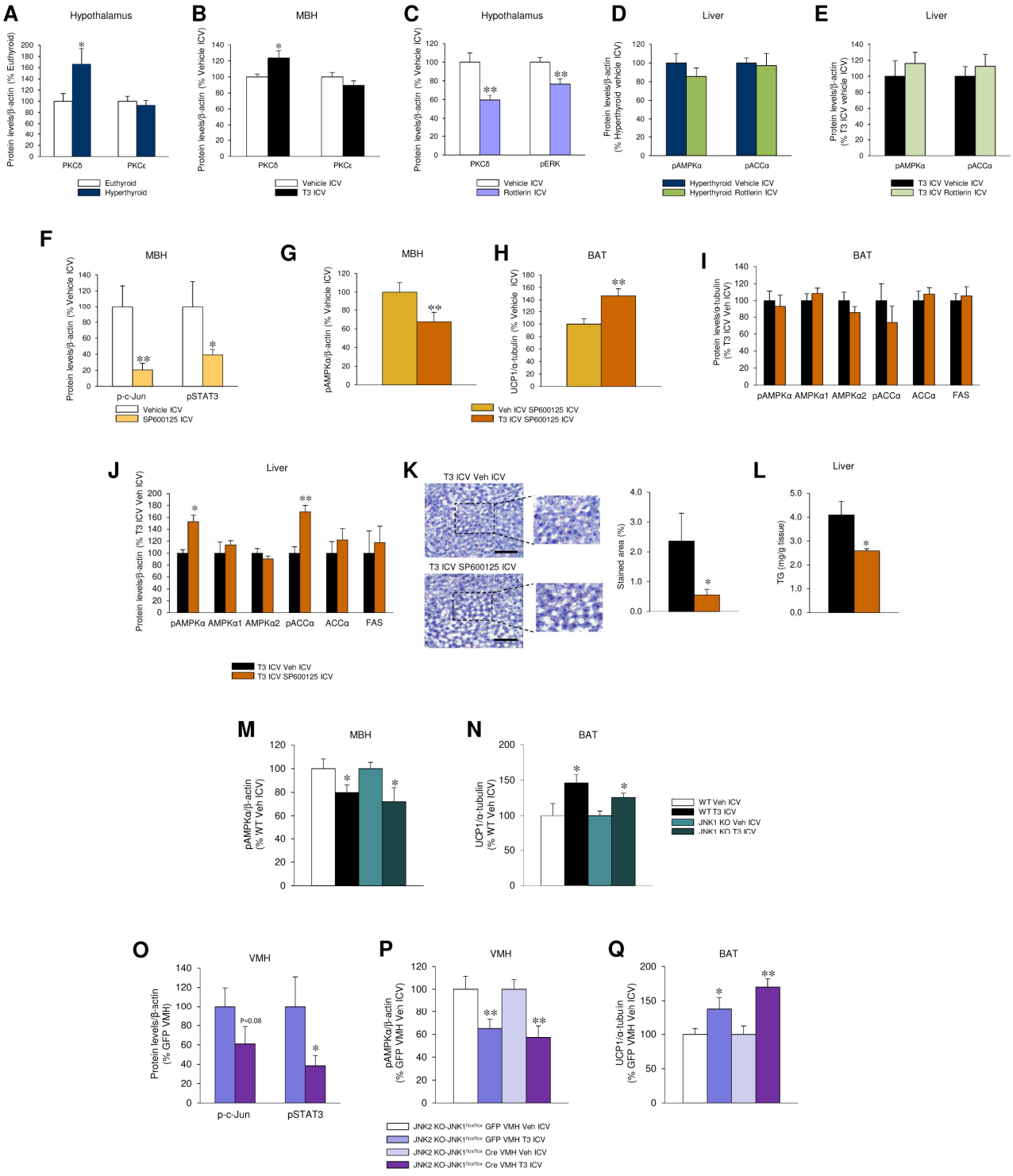

FIGURE S7 related to Figure 7. Effect JNK1 in the VMH on the central actions of T3 on liver and BAT metabolism

(A) Protein levels of PKCδ and PKCε in the hypothalamus of euthyroid and hyperthyroid rats (n=7 rats/group).

(B) Protein levels of PKCδ and PKCε in the mediobasal hypothalamus (MBH) of rats ICV treated with vehicle or T3 (n=7 rats/group).

(C) Protein levels of PKCδ and PKCε in the hypothalamus of rats ICV treated with vehicle or the PCK inhibitor rottlerin (n=7 rats/group).

(D) Protein levels of pAMPKα and pACCα in the liver of hyperthyroid rats ICV treated with vehicle or rottlerin (n=7 rats/group).

(E) Protein levels of pAMPKα and pACCα in the liver of rats ICV treated with vehicle or T3 and also with vehicle or rottlerin (n=7 rats/group).
(F) Protein levels of p-c-Jun, pSTAT3 in the MBH of rats ICV treated with vehicle or the JNK inhibitor SP600125 (n=7 rats/group).
(G-H) Protein levels of pAMPKα in the MBH **(G)** and UCP1 in the BAT **(H)** of rats ICV treated with vehicle or T3 and SP600125 (n=7 rats/group).
(I) Protein levels of the AMPK pathway in the BAT of rats ICV treated with T3 and vehicle or SP600125 (n=7 rats/group).
J) Protein levels of AMPK pathway in the liver, **(K)** representative Oil Red O images (left panel; 20x; scale bar: 100 µm), staining analysis (right panel) and **(L)** triglyceride (TG) levels in the liver of rats ICV treated with T3 and vehicle or SP600125 (n=7-8 rats/group).
(M-N) Protein levels of pAMPKα in the MBH **(M)** and UCP1 in the BAT **(N)** of *jnk1* null (JNK1 KO) and wildtype (WT) mice ICV treated with vehicle or T3 (n=4-6 mice/group).
(O-Q) Protein levels of p-c-Jun, pSTAT3 **(O)**, pAMPKα in the VMH **(P)** and UCP1 in the BAT **(Q)** of *jnk2* null-*jnk1 floxed* (JNK2 KO-JNK1$^{flox/flox}$) ICV treated with vehicle or T3 and treated in the VMH with AAV encoding GFP or Cre (n=5-7 mice/group).
**P*<0.05, ***P*<0.01, *vs.* euthyroid, vehicle ICV (in the mice experiments for both genotypes), vehicle ICV SP600125 ICV or T3 ICV vehicle ICV. All data are expressed as mean±SEM.

TABLE S1. Primers and probes for real-time PCR (TaqMan) analysis related to STAR Methods

Protein	Gene	GenBank accession number		Sequence
ACER1	*Acer1*	NM_001106875	Fw Primer	5'-CTCATCTTTGGACCCCTCATGA-3'
			Rv Primer	5'-CCATGAAGAGGACTGACACTCCAT-3'
			Probe	FAM-5'-CTTATGCACCCGTATGCCCAGAAGCG-3'-TAMRA
ADBR3	*Adrb3*	NM_013108	Fw Primer	5'-TGCTAGATCTCCATGGTCCTTCA-3'
			Rv Primer	5'-AAATCACCGCTGAACAGGTTTGATGCC-3'
			Probe	5'-TCCCTTACGGACAGCTTACCTTT-3'
AMPKα1	*Prkaa1*	NM_001013367	Fw Primer	5'- GTACCAGGTCATCAGTACACCATCT-3'
			Rv Primer	5'- GTCCAACCTTCCATTTTTACAGA-3'
			Probe	FAM-5'-TGGTGATGGAATATGTCTCTGG-3'-TAMRA
CDIPT	*Cdipt*	NM_138899	Fw Primer	5'-GAACTCTTCTACTGCCTCCTGTACCT-3'
			Rv Primer	5'-TCGGAAAAGCCCCACAGA-3'
			Probe	FAM-5'-TTCAATTTCTCCGAGGGACCACTAGTCGG-3'-TAMRA
COX1	*mt-Co1*	NC_001665.COX1.0	Assay ID	Applied Biosystems TaqMan Gene Expression Assays Assay ID Rn03296721_s1
COX4	*Cox4i1*	NM_017202.1	Assay ID	Applied Biosystems TaqMan Gene Expression Assays Assay ID Rn00567950_m1
CPT1a	*Cpt1a*	NM_031559.1	Fw Primer	5´-ATGACGGCTATGGTGTCTCC-3
			Rv Primer	5´-TCATGGCTTGCTTCAAGTGC-3´
			Probe	FAM-5´-TGAGACAGACTCACACCGCT-3´-TAMRA
CPT1b	*Cpt1b*	NM_013200.1	Assay ID	Applied Biosystems TaqMan Gene Expression Assays Assay ID Rn00566242_m1
DGAT1	*Dgat1*	NM_053437	Fw Primer	5'-TTCCGCCTTTGGGCATTC-3'
			Rv Primer	5'-TTGGAAGAAGCGGTTCACAATC-3'
			Probe	FAM-5'-CAGCAATGATGGCTCAGGTCCCACTG-3'-TAMRA
DIO2	*Dio2*	NM_031720.3	Assay ID	Applied Biosystems TaqMan Gene Expression Assays Assay ID Rn00581867_m1
FABP3	*Fabp3*	NM_024162.1	Fw Primer	5'-ACGGAGGCAAACTGGTCCAT-3'
			Rv Primer	5'-CACTTAGTTCCCGTGTAAGCGTAGTC-3'
			Probe	FAM-5'-TGCAGAAGTGGGACGGGCAGG-3'-TAMRA
FGF21	*Fgf21*	NM_130752.1	Assay ID	Applied Biosystems TaqMan Gene Expression Assays Assay ID Rn00590706-m1
GLUT1	*Slc2a1*	NM_138827.1	Assay ID	Applied Biosystems TaqMan Gene Expression Assays Assay ID Rn01417099_m1
HSL	*Lipe*	NM_012859.1	Fw Primer	5'-CCAAGTGTGTGAGCGCCTATT-3'
			Rv Primer	5'-TCACGCCCAATGCCTTCT-3'
			Probe	FAM-5'-AGGGACAGAGACGGAGGACCATTTTGACTC-3'
HPRT	*Hprt*	NM_012583	Fw Primer	5'-AGCCGACCGGTTCTGTCAT-3'
			Rv Primer	5'-GGTCATAACCTGGTTCATCATCAC -3'
			Probe	FAM-5'-CGACCCTCAGTCCCAGCGTCGTGAT 3'-TAMRA
LASS1	*Cers1*	NM_001044230	Fw Primer	5'-TGCTCCTCCTGGTCATGAACAT-3'
			Rv Primer	5'-CAAGTCTTCCAGTTCACGCATCT-3'
			Probe	FAM-5'-CTGGTTCCTGTACATTGTGGCTTTTGCAGC-3'-TAMRA
LIPIN1	*Lpin1*	NM_001012111	Fw Primer	5'-CCTCTACTTCTGGCGATGCA-3'
			Rv Primer	5'-CATCTTATCTCTCATGATGGATTCC-3'
			Probe	FAM-5'-TCCAGAAACCTTTGCCAAAGGCCA-3'-TAMRA
LPL	*Lpl*	NM_012598.2	Fw Primer	5'-TGGAGAAGCCATCCGTGTG-3'
			Rv Primer	5'-TCATGCGAGCACTTCACCAG-3'

			Probe	FAM-5'- TGCAGAGAGAGGACTCGGAGACGTGG-3'-TAMRA
NRF1	*Nrf1*	NM_001100708.1	Fw Primer	5´-TGTTTGGCGCAGCACCTTT-3´
			Rv Primer	5´-CGC AGA CTC CAG GTC TTC CA-3´
			Probe	FAM-5´- ATGTGGTGCGCAAGTACAAGAGCATGATC3´-TAMRA
PCYT1a	*Pcyt1a*	NM_078622.2	Assay ID	*Applied Biosystems TaqMan Gene Expression Assays* Assay ID Rn00589584_m1
PGC1α	*Ppargc1a*	NM_031347	Fw Primer	5'-CGATCACCATATTCCAGGTCAAG-3'
			RvPrimer	5'-CGATGTGTGCGGTGTCTGTAGT -3'
			Probe	5'-AGGTCCCCAGGCAGTAGATCCTCTTCAAGA -3'
PGC1β	*Ppargc1b*	NM_176075.2	Assay ID	Applied Biosystems TaqMan Gene Expression Assays Assay ID Rn00598552_m1
PISD	*Pisd*	XM_001061408	Fw Primer	5'-TTCTTCCGGCGTAAGCTGAA-3'
			Rv Primer	5'-CCTGCCCAAAGGTGAGGAT-3'
			Probe	FAM-5'-CTGTCTGTGGCTTGCACAGTGTGATCAGC-3'-TAMRA
PLA2g4a	*Pla2g4a*	NM_133551	Fw Primer	5'-TTGGATTGTGCGACCTACGTT-3'
			Rv Primer	5'-GGGTGGGAGTACAAGGTTGACA-3'
			Probe	FAM-5'-CTGGTCTGTCCGGCTCCACATGGTA-3'-TAMRA
PNPLA2	*Pnpla2*	NM_001108509	Fw Primer	5´-CCGCTGGAGAGTGCAGTGT-3´
			Rv Primer	5´-CACCGGATATCTTCAGGGACAT-3´
			Probe	FAM-5'-CACCATCCGCTTGTTGGAGTGGC-3´-TAMRA
			Probe	FAM-5'-CTGCAAGGGCTTCTTTCGGCGA-3'-TAMRA
PPARγ	*Pparg*	NM_013124	Fw Primer	5'-TGGGCCAGAATGGCATCTC-3'
			Rv Primer	5'-CTGATGCACTGCCTATGAGCACTTCACA-3'
			Probe	FAM-5'-CTAACTCCCAGAAAAGCAAGCAA-3'-TAMRA
PRDM16	*Prdm16*	NM_001177995.1	Assay ID	*Applied Biosystems TaqMan Gene Expression Assays* Assay ID Mm01266512_m1
PTDSS1	*Ptdss1*	NM_001012113	Fw Primer	5'-ATGGTCGTTTGCCGGTTTT-3'
			Rv Primer	5'-CCCTGTGGTGGTGTGGATGT-3'
			Probe	FAM-5'-ATGAGGACTTACCACTGGGCAAGCTTCAAG-3'-TAMRA
SGMS1	*Sgms1*	NM_181386	Fw Primer	5'-CGGCATGCACTTCAACTGTT-3'
			Rv Primer	5'-ATTATCCTCCGCACTTGAGCTT-3'
			Probe	FAM-5'-CCGAAGCTCTTTGGAG-3'-TAMRA
SMPD2	*Smpd2*	NM_031360	Fw Primer	5'-CACCTACCCGGATGCACACT-3'
			Rv Primer	5'-GATTGGGTGTCTGGAGAACACA-3'
			Probe	FAM-5'-TTCAGAAGCGGAATCATTGGCAGTGG-3'-TAMRA
SPTLC1	*Sptlc1*	NM_001108406	Fw Primer	5'-TGACCTGGAGCGACTGCTAA-3'
			Rv Primer	5'-CCTTCCGCGACGATGAAT-3'
			Probe	FAM-5'-CAAAAGAATCCTCGAAAGGCCCGTG-3'-TAMRA
TFB1M	*Tfb1m*	NM_181474.2	Assay ID	Applied Biosystems TaqMan Gene Expression Assays Assay ID Rn00710690_m1
TFB2M	*Tfb2m*	NM_001008293.1	Assay ID	Applied Biosystems TaqMan Gene Expression Assays Assay ID Rn01412504_m1
UCP1 (rat)	*Ucp1*	NM_012682	Fw Primer	5'-CAATGACCATGTACACCAAGGAA-3'
			Rv Primer	5'-GATCCGAGTCGCAGAAAAGAA-3'
			Probe	FAM-5'-ACCGGCAGCCTTTTTCAAAGGGTTTG-3'-TAMRA
UCP1 (mouse)	*Ucp1*	NM_009463	Fw Primer	5'-CGATGTCCATGTACACCAAGGAA-3'
			Rv Primer	5'-GACCCGAGTCGCAGAAAAGAA-3'
			Probe	FAM-5'-ACCGACGGCCTTTTTCAAAGGGTTTG-3'-TAMRA
UCP3	*Ucp3*	NM_013167.2	Assay ID	Applied Biosystems TaqMan Gene Expression Assays Assay ID Rn00565874_m1